AIMS Materials Science, 12(1): 1–22.
DOI: 10.3934/matersci.2025001
Received: 30 October 2024
Revised: 02 January 2025
Accepted: 09 January 2025
Published: 13 January 2025

http://www.aimspress.com/journal/Materials

Review

Laser surface processing technology for performance enhancement of TENG

Jia Tian[1,2,†], Yue He[1,2,†], Fangpei Li[1,2,*], Wenbo Peng[1,2,*] and Yongning He[1,2,*]

[1] School of Microelectronics, Xi'an Jiaotong University, Xi'an, Shaanxi, 710049, China
[2] The Key Lab of Micro-Nano Electronics and System Integration of Xi'an City, Xi'an, Shaanxi, 710049, China
[†] These authors contributed equally to this work.

* **Correspondence:** Email: lifangpei@xjtu.edu.cn; wpeng33@mail.xjtu.edu.cn; yongning@mail.xjtu.edu.cn.

Abstract: The triboelectric nanogenerator (TENG), as a new energy harvesting device, can efficiently harvest mechanical energy from the environment to provide continuous power for electronic devices, which has great potential for powering intelligent distributed network. Laser processing technology, which enables structural, phase, and property control at different scales, can quickly and easily complete the surface patterning of TENG and facilitate efficient energy harvesting. In this work, we outline the working modes and principles of TENG, review the research progress of laser surface processing technology for fabricating TENG in recent years, including laser-induced graphene (LIG), laser ablation, laser carbonization, laser-induced copper, etc., and perspectives on the challenges and future directions for development of laser surface processing for performance enhancement of TENG.

Keywords: laser processing; triboelectric nanogenerator; laser-induced graphene; surface strategies

1. Introduction

In recent years, with the rapid progress of wireless network and mobile communication technology, the Internet of Things (IoT) has been widely emphasized and developed and will play an important role in the fields of environmental monitoring, medical and health care, smart identification,

and artificial intelligence. In the future intelligent distributed network, an effective solution to the power supply problem of each electronic node is urgent. However, traditional storage battery power solutions require frequent charging or replacement, cable transmission power supply is not applicable to most scenarios, and solar power generation is highly affected by weather conditions, which makes it impractical to ensure the normal operation of all nodes. Since most electronic devices are usually milliwatt power, distributed energy harvesting is a promising method, as it is sufficient to solve the problem of powering electronic nodes by harvesting stray energy that is dispersed in the environment and converting them into electrical energy [1]. Hence, in 2012, Prof. Zhong Lin Wang's team proposed the theory of triboelectric nanogenerator (TENG), which can utilize the coupling principle of contact electrification (CE) and electrostatic induction between materials to achieve efficient conversion from low-frequency mechanical energy to electrical energy [2]. TENG, which has the advantages of light weight, low cost, diverse structure and wide choice of materials, shows great potential for large-scale development of IoT. In addition, TENG also shows great application value in the fields of self-powered sensors [3,4], micro/nano energy [5,6], high-voltage applications [7,8], blue energy [9,10], catalysis [11,12], etc.

Nevertheless, the output of TENG is highly correlated with the generation of surface charge. Since the contact at the microscopically rough interfaces between solid materials is not tight, the micro-nanostructures on the surface of the materials lead to an increase in the effective contact area, and this results in an increase in the number of sites for charge transfer. In addition, the interfacial resistance between the electrodes and the dielectric layer of the TENG can also affect the charge transfer. To overcome the challenges above, surface modification of TENG materials is essential. As a processing technology that can be used for almost all materials, laser technology can realize the control of structure at different scales, phases, and properties, and has a remarkable performance in the fields of functional surfaces and electronic devices [13–15]. In recent years, there have also been some relevant studies on the use of laser technology for performance enhancement of TENG [16–20], but a systemic summary and integration to the application of laser surface processing technology in the field of TENG is lacking. Therefore, the recent advances and developing methods of laser processing in the field of TENG are comprehensively reviewed and well organized in this paper as follows. In Section 1, we introduce the background and significance. In Section 2, we describe the working modes and principles of TENG and explain the necessity of TENG surface modification and the merits of surface laser processing for performance enhancement of TENG. In Section 3, we review some strategies of surface laser processing and its applications in TENG, including laser-induced graphene (LIG), laser ablation, laser carbonization, laser-induced copper, and other techniques. Finally, in Section 4, we discuss the challenges and future perspectives in related fields.

2. Necessity of laser surface processing on TENG

2.1. Working modes and operating principles of TENG

Before the introduction of laser surface processing technology, it is of great significant to look at the basic working modes and operating principles of TENG. According to the different ways of generating and collecting electric energy during operation, TENG can be divided into four working modes, as shown in Figure 1: (1) Contact-Separation Mode TENG (CS-TENG), (2) Lateral Sliding Mode TENG (LS-TENG), (3) Single-electrode Mode TENG (SE-TENG), and (4) Freestanding

Triboelectric-layer Mode TENG (FT-TENG). Moreover, the operating principles of the four kinds of TENG above are also distinct. When CS-TENG works, both triboelectric layers are electrically neutral in the initial state. When an external force is applied to make the two layers be in close contact with each other, the charges will transfer in the contact area due to the occurrence of the contact electrification effect. When the external force is removed and the two layers are separated, under the effect of electrostatic induction, open-circuit voltage and short-circuit current will be generated between the two metal electrodes [21], as is shown in Figure 1a,b. In the case of LS-TENG, when two triboelectric layers are in close contact and sliding relative to each other, the energy generated by the friction will stimulate electron-hole pairs at the contact interface, generating triboelectric charges. These charges are collected by the circuits [22], as shown in Figure 1c,d. The working mechanism of SE-TENG is very similar to that of LS-TENG except that the triboelectric charges will increase or decrease only on the electrode connected with the load, so the direction of electron transfer will be reversed during the sliding process, and the output current is alternate instead of direct [23], as is shown in Figure 1e. Finally, FT-TENG is a kind of TENG that connects two SE-TENGs electrodes through wires to realize comprehensive power generation. In this structure, the two SE-TENGs share the same triboelectric layer. When the triboelectric layer slides, charges with different amounts will be generated on the two electrodes due to different contact areas. This will lead to a potential difference between the electrodes, driving electrons to transfer in the external circuit to generate current [24], as shown in Figure 1f. Because of the diversity of the overall structures and working modes, the four kinds of TENG above can cover most application scenarios well. For instance, TENG can be used as an energy collection device to convert various forms of mechanical energy into electrical energy and store it for power supply of electronic devices [25–29]. In addition, the voltage and current generated by TENG can also be used as electrical signals, which are widely used in the fields of self-powered sensing [30–32], human-computer interaction [33–35], and other relative fields.

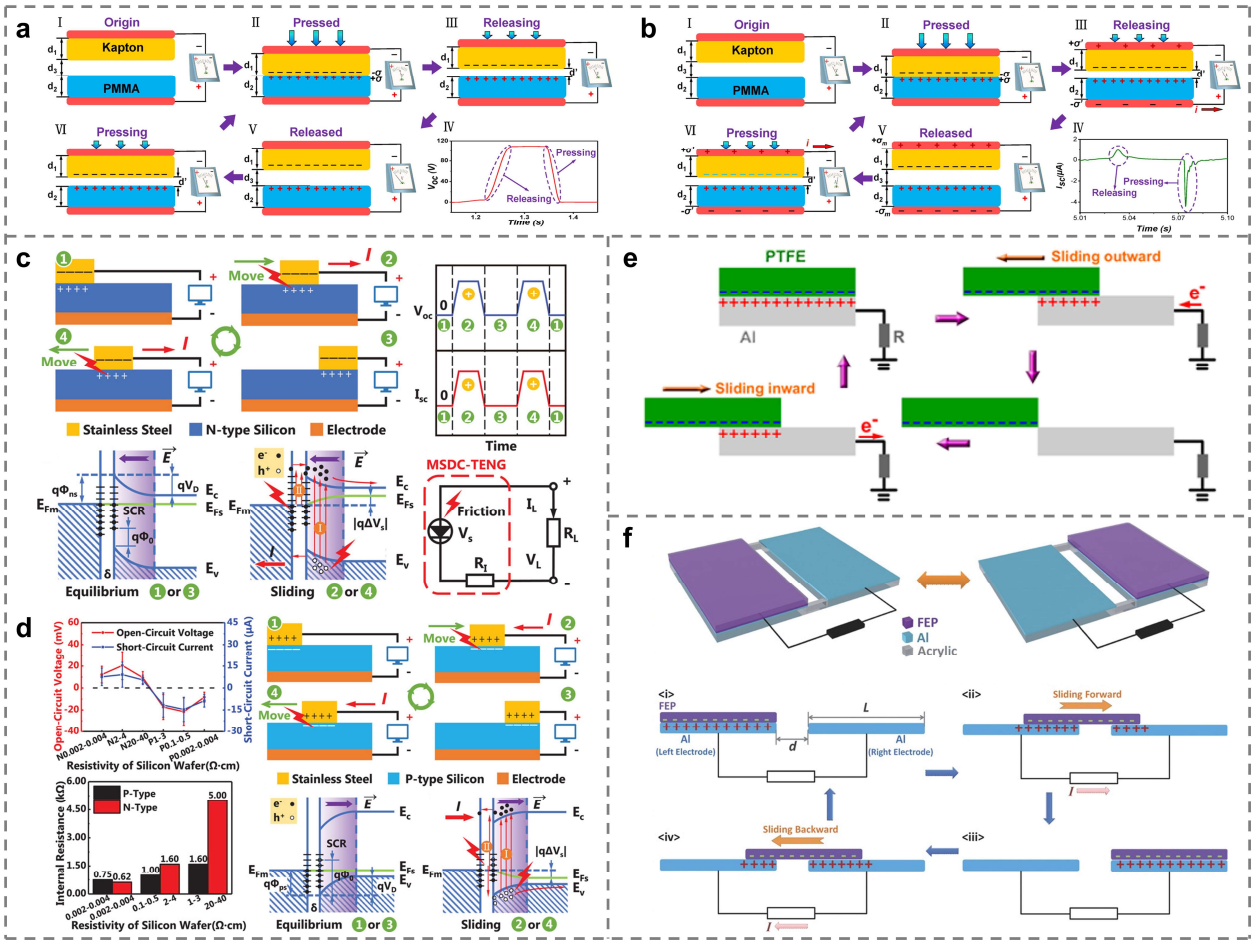

Figure 1. Four basic working modes and mechanisms of TENG. (a, b) Contact-separation mode TENG (CS-TENG) (Reproduced from Ref. [21] with permission). (c, d) Lateral Sliding mode TENG (LS-TENG) (Reproduced from Ref. [22] with permission). (e) Single-electrode mode TENG (SE-TENG) (Reproduced from Ref. [23] with permission). (f) Freestanding Triboelectric-layer mode TENG (FT-TENG) (Reproduced from Ref. [24] with permission).

2.2. Merits of laser surface processing

Due to the inherent capacitance, the output of traditional TENG is characterized by high voltage and low current, resulting in very little output power at the load [36]. Thus, after establishing a relatively complete concept and principle system of TENG, researchers gradually begin to focus on how to improve TENG's performance. Haiyang Zou's team has determined triboelectric series of many materials with liquid metal by a general standard method [37], as is shown in Figure 2a. Theoretically, if the materials that are far apart in this sequence are used as a triboelectric layer, a larger output can be obtained. However, due to the complexity of material processing, low compatibility of application scenario and high cost, this method is difficult to popularize.

Furthermore, since TENG is based on the charge transfer generated by the contact electrification effect between the surfaces of the friction layer materials, the heterogeneous charges gathered on the surfaces are subsequently harvested via electrical circuits due to electrostatic induction (for dielectrics)

and carrier migration (for conductors). We would normally infer the direction and amount of charge transfer during the contact- separation process based on the difference of the work function between the friction layers, but the spatial heterogeneity of the materials (i.e., inhomogeneities in the microstructure and properties of the material surfaces) may result in an inhomogeneous charge distribution in the form of (+/−) charge mosaics at the contacting surfaces [38–40], and thus the charge collected using the TENG device is actually a net macroscopic transfer charge. Localized heterogeneous charges may be bound by the surface state or neutralized, depending on the ability of the material to retain the charge.

During the TENG operation, the surface charge density σ plays a key role in the output of the TENG [41], and its value is mainly limited by the combination of four factors, which is shown in Eq 1 [42]:

$$\sigma_{\max,\ \text{output}} = (\sigma_{CE},\ \sigma_{AB},\ \sigma_{DB})\cdot\eta \tag{1}$$

where $\sigma_{\max,\ \text{output}}$ represents the maximum surface charge density in TENG operation, σ_{CE} represents the triboelectrification capability, σ_{AB} represents the maximum air breakdown charge density, σ_{DB} represents the maximum breakdown charge density of dielectric material, and η represents the contact efficiency between materials.

From this, it can be seen that to obtain the output of high surface charge density, it is necessary to make the material have a strong triboelectrification ability first. Different surface modifications to the friction layer materials to regulate the surface state are very important to enhance the efficiency of CE. The main research on surface engineering of friction materials is centered around two means: chemical modification and physical modification, as is shown in Figure 2b,c. Chemical modification is mainly aimed at organic materials to adjust their electron gaining or losing ability by means of changing chemical functional groups [43,44], ion injection [45,46], element doping [47,48], etc., which can improve the limitation of the surface charge density. However, not all materials are suitable or capable of being modified by functional groups; and the process sometimes requires the use of strong acids, bases, or other corrosive chemicals, which are potentially hazardous to the environment and operators; and the modification process may be more complex and involve multiple steps, making it difficult to achieve large-scale industrial applications. Physical modification is generally performed by surface patterning techniques, such as photolithography [25,49], screen printing [50,51], laser patterning [52,53], etc., to fabricate multiple micro/nano-patterned structures with regular and uniform textures on the surface of materials, to improve their contact efficiency, or to reduce their charge attenuation and thus increase their effective charge density. Physical modification usually does not involve chemical reactions, so the by-products or contamination associated with some chemical treatments can be avoided; it is also fast and suitable for most materials (including metals, ceramics, polymers, etc.), and the process can better retain the original properties of the substrate. A comparison of laser processing with other surface modification methods is shown in Table 1.

Table 1. Characteristics and comparison of surface modification methods [54,55].

Method	Applicable Materials	Processing Scale	Advantages	Disadvantages
Changing chemical functional groups	Polymer	Nanoscale	Realization of molecular level modifications to add specific functionality (e.g. hydrophilicity, corrosion resistance)	Chemical waste contamination, complex processing
Ion injection	Metal, alloy, ceramic, insulator, polymer, semiconductor	Nanoscale~microscale	Penetrating deep into the material and enhance mechanical, chemical and electrical properties	High cost, specific equipment required, complex processing
Element doping	Metal, ceramic, semiconductor	Nanoscale~microscale	Changing the chemical composition to enhance specific functions of the material (e.g., electrical conductivity, optical properties)	High-temperature processing, cumbersome processing
Photolithography	Semiconductor, metal, ceramic	Nanoscale~macroscale	High resolution (nanometer scale) for complex pattern processing	Cumbersome processing, expensive equipment required, environmental pollution, suitable for flat surfaces
Screen printing	Fabric, paper, plastic, metal, polymer, ceramic	Microscale	Simple process, suitable for mass production	Low resolution, suitable for flat surfaces only
Laser pattern processing	Metal, ceramic, polymer, composite, fabric	Nanoscale~macroscale	non-contact fabrication, fast processing speed, controllable scanning paths, 3D compatibility, excellent spatial accuracy, no need for masks	High cost, limited depth of processing

Among these methods, laser processing has obvious advantages in processing and fabricating TENG due to the advantages of non-contact fabrication, fast processing speed, controllable scanning paths, three-dimensional (3D) compatibility, excellent spatial accuracy, no need for masks, and a wide range of applicable materials.

Laser processing is categorized into continuous wave laser (CW-laser) and pulse laser based on the mode of operation of the laser source. CW-laser's energy is uniform and stable, with high average power, but the peak power is usually not high, usually at the level of hundred watts, so it is commonly used for large-area heat treatment of materials [56]; while pulse lasers, due to the length of the pulse duration ranging from

microseconds, nanoseconds, picoseconds, and femtoseconds to attoseconds, the difference between the peak power also varies greatly, but is usually much higher than that of the CW-laser, and when it acts on the surface of the material, it is easier to confine the action range to a very small area of the crystal lattice [57]. Among these laser processing methods, short-pulse laser processing represented by femtosecond laser processing is gradually favored by researchers due to its advantages of high precision, high flexibility, and mask-free processing. Since the femtosecond laser pulse duration is usually on fs level, which is smaller than the electron-phonon coupling time, and the high-power density of the femtosecond laser can cause the multi-photon absorption effect of the material, the thermal diffusion in the laser processing is thus effectively reduced, and the machining precision is high, which is suitable for the precise processing of a variety of points, lines, and layers. Based on the effect of the femtosecond laser, it has great application potential in the fields of laser ablation, reduction of graphene oxide, laser-induced graphitization, or carbonization. Due to the demands of industries, such as smart sensing, energy science, and human-machine interfaces, TENG and its related devices need to be integrated and fast-responding, etc., so laser processing, especially novel technologies such as femtosecond laser micromachining, offers a unique and promising solution to enhance the performance of TENG.

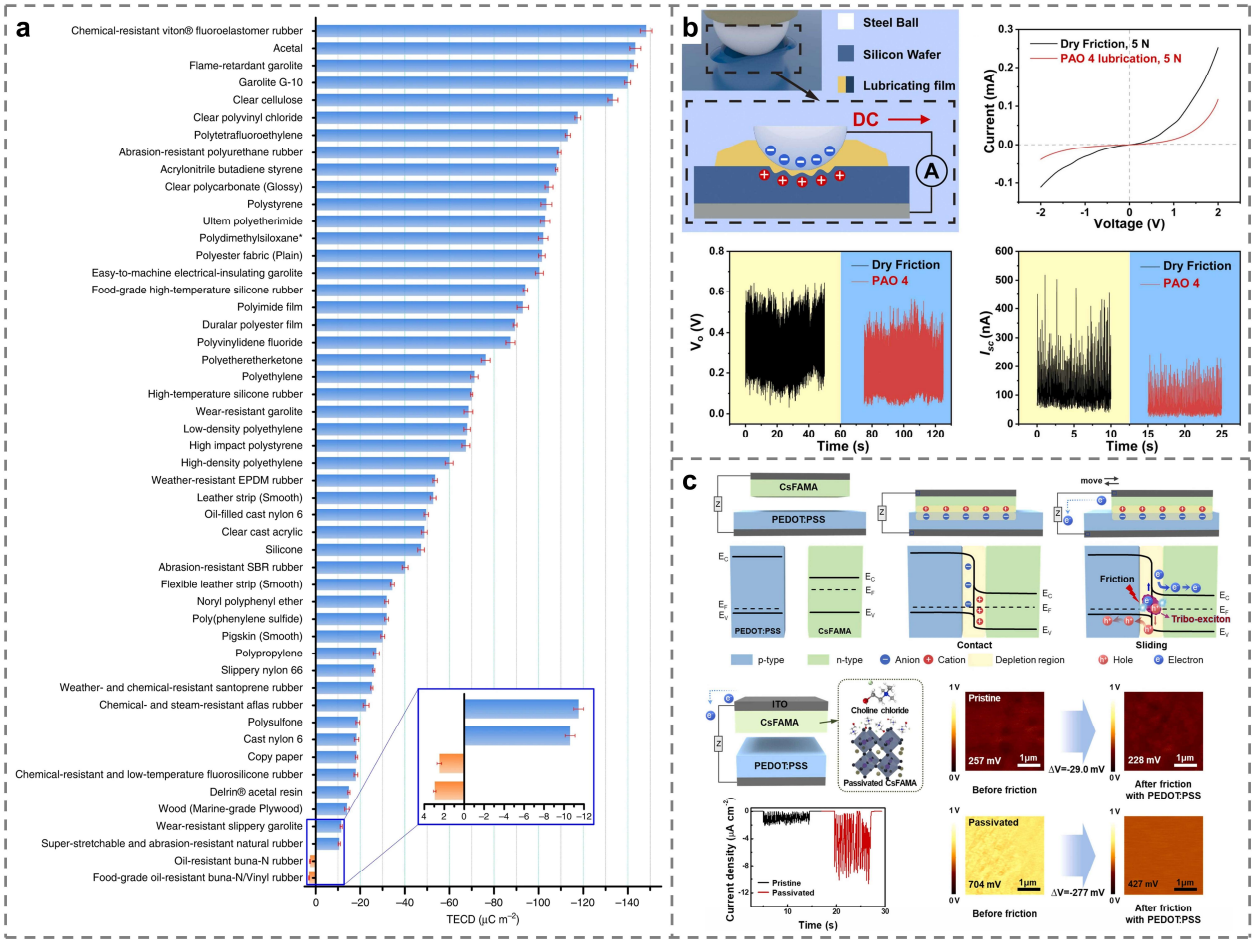

Figure 2. Different methods to enhance the performance of TENG. (a) Using materials with greater electronegativity difference (Reproduced from Ref. [37] with permission). (b) Physical strategies such as interface lubrication (Reproduced from Ref. [58] with permission). (c) Chemical strategies such as surface modification (Reproduced from Ref. [59] with permission).

3. Methods for laser surface processing of TENG

Surface laser processing is the process of irradiating the laser generated by excited radiation onto the surface of the material, so that the material absorbs the photon energy and the bond breaking, ablation, and the generation of thermal electrons in the surface area occur, thus changing the surface properties of the material. Among them, processes that primarily utilize the thermal effect of lasers on materials are photothermal processes, which is prevalent in laser processing, and processing methods such as laser ablation and laser sintering utilize the principle of the photothermal process; while in the laser process, the way that the breakage of the chemical bonds predominates without significant thermal effects is a photochemical process, including laser reduction, laser doping, laser graphitization, and other processing methods.

3.1. LIG

Graphene, as a novel carbon nanomaterial, has a series of unique physical and chemical properties. However, the traditional preparation method of graphene is complicated, and it is difficult to obtain graphene with a precisely patterned structure. In 2014, Jian Lin et al. used a pulsed laser emitted by a CO_2 infrared laser to irradiate polyimide (PI), which causes localized high temperatures in the internal lattice of PI due to vibrational excitations induced by photons and causes the carbon atoms to break their bonds and rearrange their bonds (the sp^3 carbon atoms converted to sp^2 carbon atoms), thus obtaining graphene with high crystallinity, which is the first report on LIG technology [60]. The atomic arrangement of LIG is slightly different from that of two-dimensional (2D) graphene: The lattice in 2D graphene is a hexagonal honeycomb lattice, whereas that of LIG consists of a large number of entagons, hexagons, and heptagons, as well as a small number of embedded tetragonals and octagons. This irregular structure, together with a large number of defects and grain boundaries, makes LIG more 'metallic' than 2D graphene, with improved charge storage capacity [61,62]. LIG technology is capable of producing graphene patterns without catalysts or masks, which is not only characterized by high efficiency and low cost, but also enables precise control of the pattern structure and wide material selectivity; thus, the number of TENG-related applications has been increasing in recent years.

LIG, as a low-resistance metal-free electrode material, is commonly used as an electrode material for TENG with good mechanical elasticity and durability performance, and shows reliable performance in flexible TENG [20,61–64]. As shown in Figure 3a–c, Jing Yan et al. prepared a PI membrane by electrostatic spinning technique and subsequently prepared a patterned LIG on the PI membrane using CO_2 laser. The LIG's film resistance as low as 0.4 Ω/sq, which acted as an effective charge transfer layer (CTL) to dramatically amplify the tribo-charge transfer, and significantly improved the TENG's output (V_{OC} of 51 V, I_{SC} of 5.5 μA, and Q_{SC} of 12 nC for TENG with a single PI-fiber membrane, and these outputs increased to 68 V, 7.5 μA, and 16 nC for TENG with the addition of LIG as the CTL), and the stability of the LIG integrated on PI-fiber membranes was also excellent (6,000 consecutive runs over a period of 20 days and the charge remained stable) [65]. In addition to the fabrication of patterned porous LIG by controlling the laser irradiation path, LIG electrodes can be fabricated into other structures. Kwang-Hun Choi et al. used a fast-defocusing method to prepare porous LIG, in short carbon fiber combined LIG (SF-LIG), and in long carbon fiber composite LIG (LF-LIG) by controlling the laser spot size and power density [62]. The LF-LIG-based TENG can obtain a high output (512 mW/m^2), which is 130 times higher than that of the porous LIG-based TENG (3.9 mW/m^2), as shown in Figure 3d,e. In addition, John Tianci Li et al. explored a simple laminated lamination method compatible with roll-to-roll processing, as shown in Figure 3f, and the paper/LIG/polyurethane (PU) TENG fabricated by the laminated method can produce an open-circuit

voltage of 450 V and a short-circuit current of 5.5 μA (Figure 3g–j) [66]. LIG, as a new laser processing technology, can fabricate graphene materials in a low-cost and environmentally friendly way, which provides a great possibility for the large-scale application of TENG, especially flexible self-powered devices, in the future. The specific parameters of the above laser processing methods and the specific data on the performance enhancement of TENG are shown in Table 2.

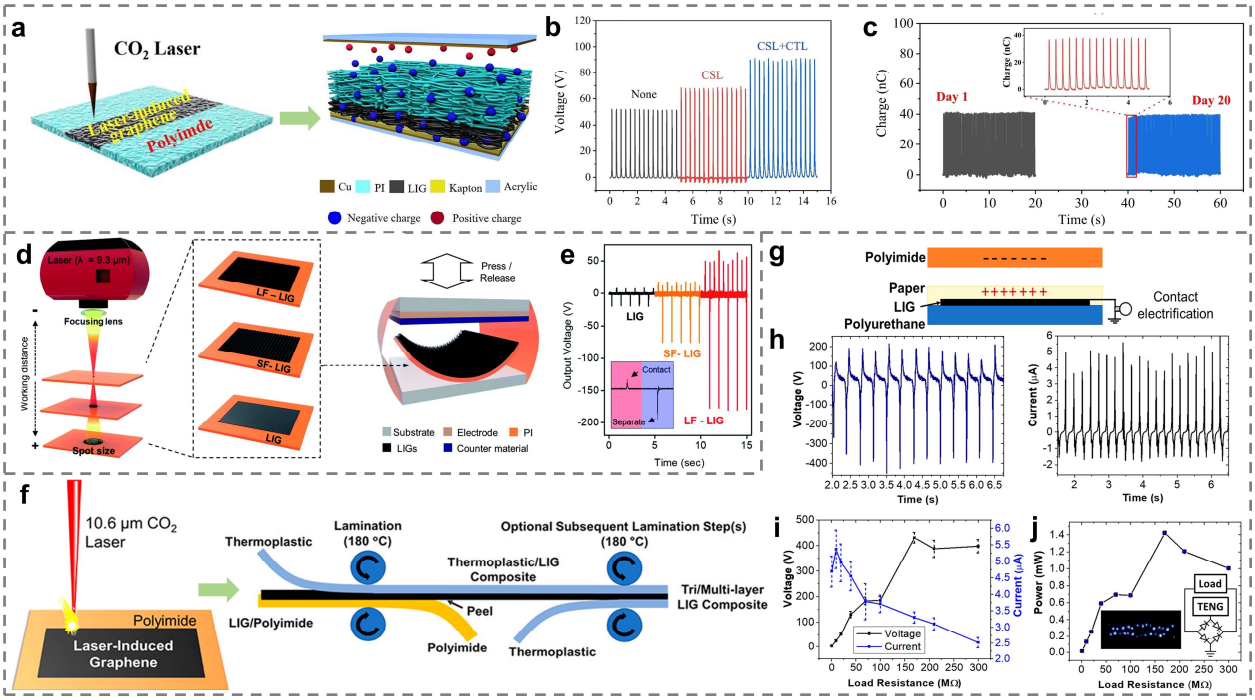

Figure 3. LIG in TENG. (a–c) LIG as CTLto enhance the performance of TENG (Reproduced from Ref. [65] with permission). (a) Schematic diagram of the laser induction process and the constructed TENG. This TENG has a LIG as CTL and a Kapton double-sided tape as charge storage layer (CSL) between the negative friction layer PI and Cu electrode. (b) V_{OC} of TENG with different functional layers. (c) The durability test of the TENG. (d, e) The TENG of structurally controlled LIG (Reproduced from Ref. [62] with permission). (d) Schematic illustration of the direct morphology controllable LIG synthesis and the fabricated press/release-type LIG based TENG. (e) Electrical output performance of different LIG (LIG, SF-LIG and LF-LIG) TENG under uniform vibrating conditions. (f–j) LIG-based TENG prepared by a lamination compositing technique (Reproduced from Ref. [66] with permission). (f) Schematic diagram of LIG synthesis on the surface of PI and the lamination process of LIG with thermoplastics. (g) Schematic and optical image for a PU/LIG/paper triboelectric device. (h) V_{OC} and I_{SC} for TENG contacted against PI. (i) Voltage and current generated as a function of load resistance. (j) Peak power generated as a function of load resistance.

Table 2. Comparison of processing parameters and enhancement of TENG's performance of LIG.

		Cu, PI/LIG [65]	PMMA, LF-LIG [62]	PI, Paper, LIG/PU [66]
Processing Parameters	Types of laser	CO_2 continuous laser	CO_2 continuous laser	CO_2 pulsed laser
	P_{laser}	18 W	220 mW	75 W
	$v_{scanning}$	80 mm/s	5 mm/s	300 mm/s
	λ	10.6 μm	9.3 μm	10.6 μm
	W.D.		0 mm	
Processed Parts		CTL	Frictional layer and electrode	Electrode
Performance and improvement ratio	V_{OC}	90 V 32.4%	180.8 V 822.4%	450 V
	I_{SC}	10.5 μA 40%		5.5 μA
	Q_{SC}	19 nC 25%		

3.2. Laser ablation

Laser ablation is a processing method that utilizes thermal or other physical effects (e.g., direct cutting of molecular or atomic bonds) to remove material atoms under strong laser irradiation, thereby altering the material's morphology and properties. Compared with etching processes such as chemical etching, surface replication, ion implantation, and photolithography, the laser ablation process has obvious advantages: it has simple equipment requirements and can be applied to almost any kind of material and can realize controllable fabrication of surface micro/nano structures of materials by controlling the laser parameters (including photon energy, power, pulse duration, and repetition frequency) [67] and the position of the laser beam [68,69]. The preparation of friction layer materials with surface patterns/surface microstructures by laser ablation can effectively increase the contact area, which has a significant effect on the improvement of TENG performance [70,71]. In the selection of the laser source, the difference between long-pulse and short-pulse lasers interacting with the material, respectively, is shown in Figure 4a. CW-laser or conventional long-pulse lasers are commonly used for large-scale, low-cost fabrication of laser surface textures due to significant thermal effects, large heat-affected zones, and defects such as rough ablation edges and microcracks, which can lead to poor quality of the surface structures obtained by ablation [18,72]. If one chooses to use a short-pulse laser, the thermal diffusion length is much smaller than the light penetration length, which will result in the laser injected energy not being able to diffuse in time before the processed area quickly reaches the vaporization temperature and ejects out of the material surface, resulting in fewer defects, better quality surface structures, and higher resolution. As shown in Figure 4b,c, Daewon Kim et al. ablated ordered microstructures on the surface of PDMS by ultrafast laser, which resulted in more than 2 times the increase in the output power of this PDMS-based TENG [73]. As shown in Figure 4d–f, Hyunwoo Cho et al. used the PI film obtained by direct UV laser ablation to prepare film-sponge-coupled TENG (FS-TENG), and the optimized open-circuit voltage and short-circuit current reached 48.19 V

and 1.243 μA, respectively, which is a 3 times increase in the electrical performance over the unoptimized FS-TENG, and it has an excellent durability, with a degradation rate of less than 3% after 50,000 cycles [74]. Ji Huang et al. used femtosecond laser scanning ablation to prepare micro/nano dual-scale structures in stripes and cones by ablation on the surface of a copper film and compared it with PDMS having micro-nano structures obtained by ablation to construct TENG, as shown in Figure 4g–j: the TENG's power density was 21 times higher than that of TENG without micro-nano structures [75]. Laser ablation provides a unique and effective solution to improve the performance of TENG by precisely designing and ablating the surface patterns of different materials, which can increase the contact area of friction materials and optimize the surface conditions. The specific parameters of the above laser processing methods and the specific data on the performance enhancement of TENG are shown in Table 3.

Table 3. Comparison of processing parameters and enhancement of TENG's performance of laser ablation.

		Al, LI-PDMS, Al [73]	SRPA sponge, PI (H-sq) [74]	Cu PDMS [75]	
Processing parameters	Types of laser	Femtosecond pulsed laser	UV laser	Femtosecond pulsed laser	
	Processing mode	Single laser pulse		Multi-fast laser scanning and single-low laser scanning for Cu	Single laser pulse for PDMS
	F_{laser}			5.38 J/cm^2	
	P_{laser}	29 mW	10 W		8 mW
	$v_{scanning}$	100 mm/s	150 mm/s	2 mm/s 0.2 mm/s	
	λ	1030 nm	354.7 nm	800 nm	800
	f	10 kHz	30 kHz		
	Δt	210 fs	14 ns	143 fs	143 fs
Processed parts		Frictional layer	Frictional layer	Frictional layer and electrode	Frictional layer
Performance and improvement ratio	V_{OC}	42.5 V 32.8%	48.19 V 186.5%	22.04 V 312.7%	
	I_{SC}	10.1 μA 44.3%	1.243 μA 139%	2.6 μA 409.8%	
	Q_{SC}			7.69 nC 357.7%	
	P_{max}	1073 mW/m^2	98.95 mW/m^2	210 mW/m^2 2000%	

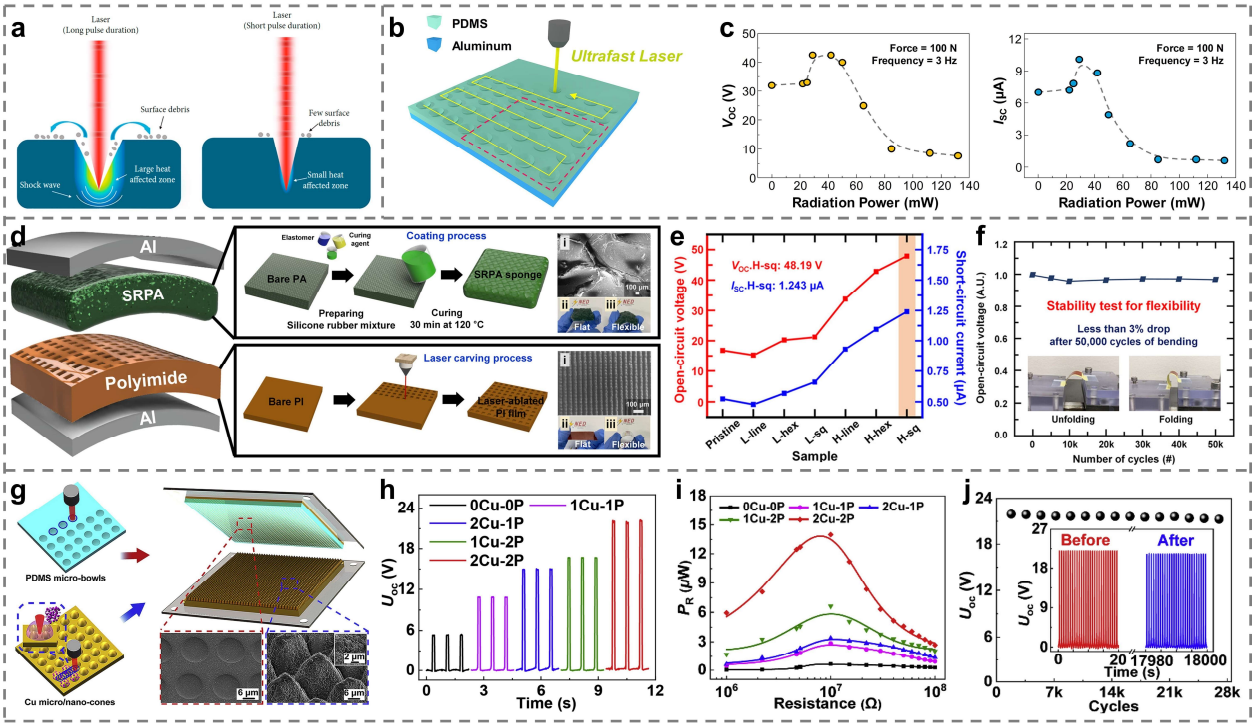

Figure 4. Laser ablation in TENG. (a) Illustration of laser–matter interaction characteristics (the gradient color represents the heat affected zones) (Reproduced from Ref. [57] with permission). (b, c) Preparation and properties of PDMS-based by laser ablation (Reproduced from Ref. [73] with permission). (b) Schematic illustration of the fabrication of the LI-PDMS by ultrafast laser irradiation. (c) V_{OC} and I_{SC} of the fabricated LI-TENG with laser power levels ranging from 0 to 132 mW. (d–f) Film-sponge-coupled TENG (FS-TENG) based on Pi film prepared by laser ablation (Reproduced from Ref. [74] with permission). (d) Configuration of the FS-TENG and fabrication process. (e) V_{OC} of six types of the laser-ablated PI films and the pristine PI film. (f) Long-term durability test of flexible property of FS-TENG device. (g–j) Micro/nano-structures-enhanced TENG by femtosecond laser direct writing (Reproduced from Ref. [75] with permission). (g) Schematic diagrams for fabrication process, structure and SEM images of micro/nano-structured triboelectric nanogenerator. (h) U_{OC} of the TENG with different micro/nano-structures. (i) Calculated instantaneous powers of the TENG on variable resistances. (j) Stability of the TENG, inset shows the U_{OC} of the TENG before and after 5 h at 1.5 Hz.

3.3. Other laser processing methods

In addition to laser-induced graphene and laser ablation, other laser processing modes have been reported in the field of TENG. For instance, Md Salauddin et al. used laser-carbonized (LC)-MXene/ZiF-67 nanocomposites as the interlayer of non-contact mode TENG (NCM-TENG), and the larger surface area and higher charge trapping performance significantly improved the performance of this TENG, as shown in Figure 5a–d [76]. Shunli Zhu et al. used femtosecond laser direct writing technique to induce copper oxide reduction to realize the preparation of TENG patterned laser-induced copper (LIC) electrode as shown in Figure 5e–g. The fabricated LIC electrodes have a high resistivity of 0.4 Ω/sq, a good mechanical durability, and a long-term stability of more than 20 weeks, and the fabricated TENG also has a high resistivity of 0.4 Ω/sq, good mechanical durability, and long-term stability of more than 20 weeks under the high performance with low-frequency mechanical energy

input (V_{OC} of 200 V, I_{SC} of 27.4 μA, and P_{max} of 3.0 W/m^2) [77]. The specific parameters of the above laser processing methods and the specific data on the performance enhancement of TENG are shown in Table 4.

Table 4. Comparison of processing parameters and enhancement of TENG's performance of other laser processing methods.

		Laser-carbonized (LC)	LIC
Materials		Mxene, silicone, LC-MXene/ZiF-67 nanocomposite [76]	Nylon, PVDF-TrFE, LIC [77]
Processing parameters	Types of laser	CO_2 laser	CO_2 laser
	P_{laser}	1.8 W	5 W
	$v_{scanning}$	58.42 mm/s	30 mm/s
	λ	10.6 μm	10.6 μm
Processed parts		Intermediate layer	Electrode
Performance	V_{OC}	35 V	200 V
	I_{SC}	12.5 μA/m^2	27.4 μA
	Q_{SC}		98 nC
	P_{max}	55 mW/m^2	3000 mW/m^2

Besides the techniques used in the above studies, laser cutting is also commonly used for the processing of TENG surface structures. As shown in Figure 5h, Youchao Qi et al. used laser cutting to process a kirigami structure with one or two-degrees-of-freedom as a friction layer and investigated in detail the frequency response characteristics of this kirigami-inspired TENG with respect to the mass, acceleration, and initial distance and optimized its structural design [78]. Siju Mishra et al. reported a laser printing technique to print different line patterns on the friction layer increasing the friction area (Figure 5i), which increased the open-circuit voltage (~420 V) by an increase of ~11 times, and the short-circuit current density (~83.33 mA/m^2) by an increase of ~17 times [79]. In addition, Seoungwoong Park et al. utilized a photonic thermal decomposition mechanism to synthesize two-dimensional MoS_2 (Figure 5j) using a laser directed synthesis by adjusting the energy of the irradiated laser to tailor the crystal morphology and apply internal stresses, which resulted in the surface-pleated MoS_2 TENG device with approximately 40% higher power than that of the planar MoS_2 devices [80].

Other laser processing methods such as selective laser sintering and laser reduction of graphene oxide are less popular in the fabrication of TENG. Selective laser sintering (SLS) is the process of combining multiple nanoparticles together to form a mesh structure using the photothermal effect, which belongs to the process of additive manufacturing. During processing, the laser rasterizes over the powder bed. When the local temperature is higher than the melting temperature (T_m), the powder undergoes melting, followed by cooling and recrystallization. Then, the next layer of powder is applied along the print bed. Selective sintering of the surface structure is achieved by repeating the above process. The resolution of the SLS and the surface roughness of the product depend strongly on the particle size of the powder. If the particle size is large, the spatial resolution will be reduced and the surface quality will deteriorate. Since layer deformation, microstructural aggregation, ballooning effect, microvoiding, etc. may occur during SLS, which also affects the surface roughness and the quality of the material, the application of SLS in TENG is limited [81–83].

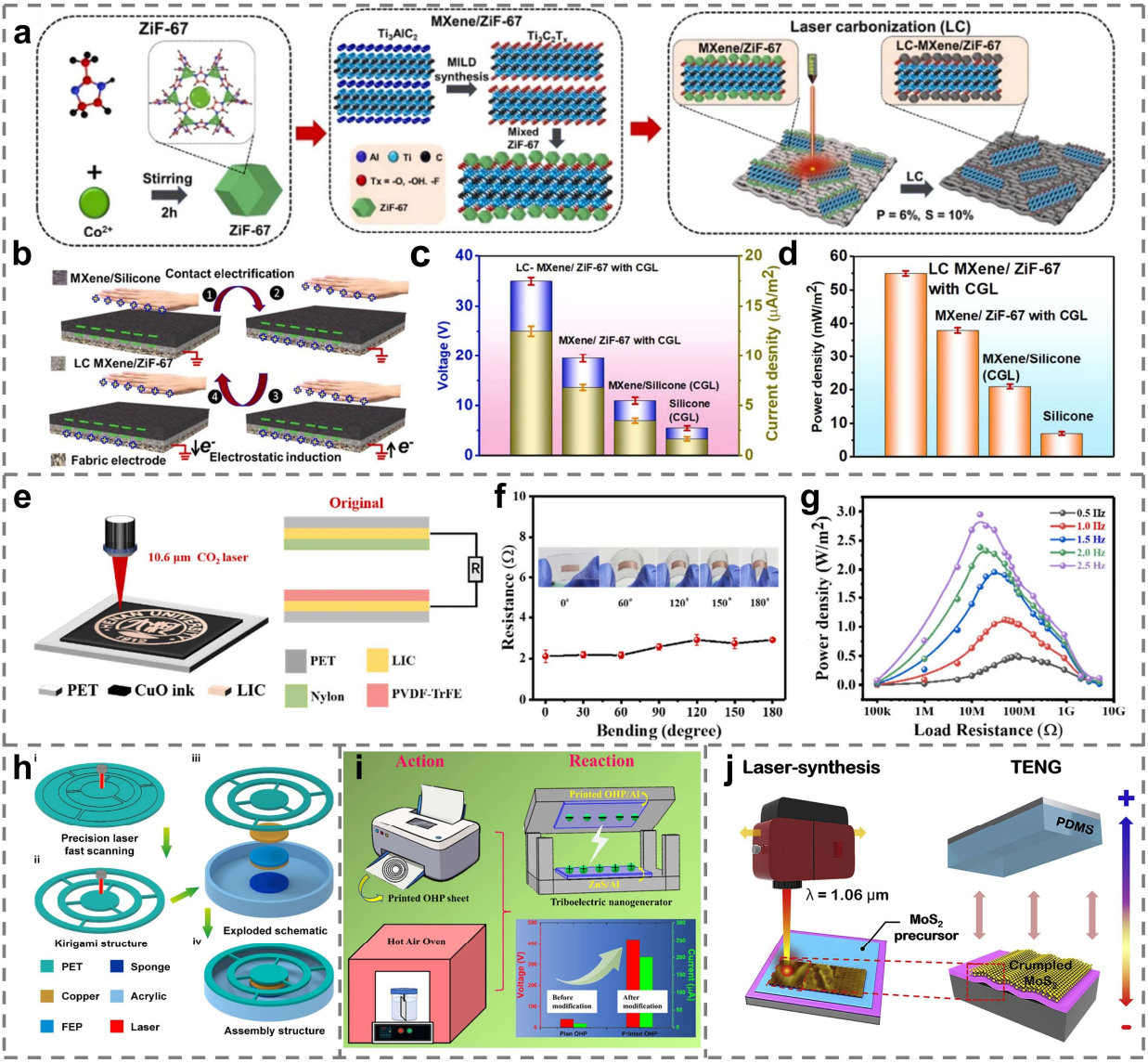

Figure 5. Other laser processing methods in TENG. (a–d) Laser-carbonized (LC)-MXene/ZiF-67 nanocomposite as an intermediate layer for boosting the output performance of TENG (Reproduced from Ref. [76] with permission). (a) Schematic representation of the fabrication of ZiF-67, MXene, and LC-MXene/ZiF-67 nanocomposites. (b) Diagram of the working mechanism of LC-MXene/ZiF-67 nanocomposite-based TENG. (c, d) Voltage, current density (c) and power density (d) performance comparisons of NCM-TENG using different materials. (e–g) TENG based on patterned laser-induced copper electrodes (Reproduced from Ref. [77] with permission). (e) Fabrication of the LIC electrode and schematic illustration of working principles of LIC-TENG. (f) Resistances of LIC at different bending angle. (g) Instantaneous power of different contact frequencies at various external load resistances. (h) Precision laser fast scanning processes for preparing the kirigami-inspired TENG (KI-TENG) (Reproduced from Ref. [78] with permission). (i) Schematic of the preparation process of TENG with laser-printed line patterns and its output properties (Reproduced from Ref. [79] with permission). (j) Schematic illustration of laser-directed synthesis of 2D MoS_2 and illustration of MoS_2-based TENG devices structures (Reproduced from Ref. [80] with permission).

Laser reduction of graphene oxide, as one of the best methods to prepare graphene in the laboratory, has rarely been reported in the field of TENG. Graphene oxide (GO) is irradiated by laser and undergoes a series of complex processes to obtain reduced graphene oxide (rGO). rGO has a high specific surface area, high electrical conductivity, and unique electro-optical properties, which may have a broad application prospect in the field of TENG in the future. For example, rGO can be used to fabricate a CTL for TENG, which can enhance the output performance of TENG by rapidly transferring the surface charge to the substrate and improving the charge transfer efficiency of the friction pairs [65]. However, the conductive properties of the prepared rGO layer may be poor due to insufficient reduction or reoxidation after reduction. Further exploration of the laser reduction process, such as controlling the parameters of laser wavelength, laser power, pulse frequency, scanning speed, and the number of laser irradiations, is needed to obtain electrode or friction materials with excellent electrical and mechanical properties [57,84].

Laser processing in TENG fabrication cannot only change the surface morphology of the materials, but may also cause changes in the trap state of the material surface, which is likewise an important factor worthy of in-depth discussion. It is crucial to control the surface roughness and microscopic morphology of the material during laser processing. With proper surface topography control, the contact area can be enhanced, thus increasing the channels for contact charge transfer. In addition, high-power laser processing may induce the introduction of more trap states, which play an important role in the charge transfer process. Surface trap states can act as temporary storage sites for charge accumulation. Among them, traps can be categorized into deep traps and shallow traps according to the trap energy level: deep trap carriers are easy to trap but not easy to release, and shallow trap carriers are easy to release but not easy to trap. The presence of surface trap states can affect the charge neutralization process, for example, free electrons may collide with trapped electrons to ionize to undergo de-trapping. If we control the surface of a friction layer material with positive friction electrode properties to trap and retain positive charges more easily while controlling the rapid neutralization of localized negative charges through the structural design of the laser processing, then its net transfer of charge in contact electrification will be greater. This requires a greater understanding of the laser-material interaction. If these mechanisms are clarified, it is believed that they can be important for the development of laser processing and TENG.

4. Conclusions and prospects

TENG, as a new energy harvesting device, has great potential for application in the future smart digital society, and the application of laser surface processing technology can enhance its performance and thus increase the possibility of large-scale application of TENG. In this review, we introduce the working modes and principles of TENG and summarize the application status of laser surface processing in the field of TENG. TENG is a device that relies on the mechanism of contact electrification and electrostatic inductive coupling to realize the conversion of low-frequency mechanical energy into usable electrical energy through the contact or sliding interfaces, and it has demonstrated a broad application prospect in the field of self-powered sensing, human-computer interaction, and other relative fields. Laser processing as a non-contact technology, which can achieve fast fabricating, controlled scanning path, high-precision processing, and a wide range of available materials, is superior to traditional technology in terms of simplicity, efficiency, scalability, controllability, high precision and eco-friendliness, etc. Moreover, processing technologies such as LIG, laser ablation, laser carbonization, laser printing, and other laser processing technologies have been successfully used in the manufacture of TENG to achieve a greatly improved of the performance.

Although considerable research progress has been made in this field, there are limitations and issues that need to be addressed.

First, technology maturity, processing efficiency, and cost. Despite the excellent performance of laser processing technology in output enhancement of TENG, such a technology is in the research and experimental stage, and more practical verification and optimization are needed. The lack of technological maturity may lead to problems such as high production cost and low production efficiency, limiting the process of its commercialization and application. How to balance processing accuracy and cost to realize mass production is a significant challenge.

Second, control of thermal effects. Compatibility and interfacial stability between materials are critical to the performance of TENG. Thermal effects and chemical changes may be introduced during laser processing, causing permanent damage to the material, and thus the relevant parameters need to be rigorously controlled to ensure the long-term stability of the TENG.

Third, standardization and commercialization of products. At the current research stage, the lack of uniform standards and process flow leads to large differences in the performance of different batches of TENG, and the product yield is not satisfactory. With the development of TENG and laser processing technology, it is necessary to establish industry standards and safety specifications, which will help promote the industrialization of TENG technology and ensure consistency of product performance and market acceptance.

Last, matching structural design and practical application. The design of micro- and nano-structures is often biased towards laboratory conditions, and it is a nonnegligible issue to maintain high performance in real-world applications. Triboelectrification nanogeneration technology faces certain challenges to achieve commercial application, including cost, reliability, stability, and factors such as market demand and competition. Interdisciplinary research and technological innovation are needed to address these issues and to promote the further development and application of laser-processed TENG.

Based on the challenges above, directions for further development to promote the deep integration of laser processing technology and TENG can be predicated as follows.

First, optimized design of high-performance multi-scale surface structures. By using laser processing technology and micro- and nano-structures, such as pyramids, hemispheres, and micropillars, fabrication can be performed directly on the surface of the friction layers to change the surface morphology and significantly enhance the performance of the TENG. Future research will focus on optimizing the shape, size, and arrangement of these structures, which can further improve the open-circuit voltage, surface charge density, and output power of the TENG to achieve higher energy conversion efficiency. Moreover, the co-design of multi-scale surface structures from the nanometer to micrometer level will be achieved by optimizing laser parameters and structure design. The further development of laser processing technology is expected to realize the preparation of larger-scale and higher-precision structures and provide technical guarantee for the manufacture of better-performance TENGs.

Second, in-depth studies of the physical and chemical phenomena involved in laser processing. Physical and chemical phenomena are intertwined during laser processing. Physical processes such as photoexcitation, electron-hole pair generation, heat conduction, etc., together with chemical processes, such as photochemical and thermally induced reactions, determine the processing effect on the material. Parameters such as pulse width, intensity, and defocusing amount of the laser cause different thermal and photochemical effects in the processing. Precise control of the laser absorption rate of the material can realize the fine tuning of the surface and internal structure of the material, fabricate specific functional nanostructures and materials, and realize TENG with better performance.

Third, expanded versatility for cross-domain applications. With the advancement of laser processing technology, the design of TENG will be more multi-functional and integrated to adapt to more application scenarios, such as energy internet, biomedicine, and wireless communication. Combined with artificial intelligence technology, it can further promote the revolution of smart devices and create more application scenarios for intelligent home, environment monitoring, smart grid, and so on.

Last, production automation for industrial scale production. In order to reduce processing costs and achieve mass production and commercialization, the automation level of laser processing needs to be further advanced. In this way, the manufacturing cost of TENG based on integration and miniaturization is expected to be further controlled, promoting its commercial application.

Use of AI tools declaration

The authors declare they have not used Artificial Intelligence (AI) tools in the creation of this article.

Acknowledgements

This research was supported by the National Natural Science Foundation of China (Grant No. 62174131 and 61704135), the China Postdoctoral Science Foundation (Grant No. 2018T111055 and 2017M613138), the Postdoctoral Research Project of Shaanxi Province (Grant No. 2017BSHEDZZ30).

Author contributions

Conceptualization and methodology: Jia Tian and Yue He; investigation: Yue He; visualization: Jia Tian; writing—original draft: Jia Tian and Yue He; writing—review & editing: Jia Tian, Yue He, and Fangpei Li; supervision: Wenbo Peng and Yongning He. All authors discussed the results and reviewed the manuscript.

Conflict of interest

The authors declare no conflict of interest.

References

1. Wang ZL (2019) Entropy theory of distributed energy for internet of things. *Nano Energy* 58: 669–672. https://doi.org/10.1016/j.nanoen.2019.02.012
2. Fan FR, Tian ZQ, Wang ZL (2012) Flexible triboelectric generator. *Nano Energy* 1: 328–334. https://doi.org/10.1016/j.nanoen.2012.01.004
3. Li Y, Yu J, Wei Y, et al. (2023) Recent progress in self-powered wireless sensors and systems based on TENG. *Sensors* 23: 1329. https://doi.org/10.3390/s23031329
4. Wu Z, Cheng T, Wang ZL (2020) Self-powered sensors and systems based on nanogenerators. *Sensors* 20: 2925. https://doi.org/10.3390/s20102925
5. Shen J, Li B, Yang Y, et al. (2022) Application, challenge and perspective of triboelectric nanogenerator as micro-nano energy and self-powered biosystem. *Biosens Bioelectron* 216: 114595. https://doi.org/10.1016/j.bios.2022.114595
6. Shi Q, He T, Lee C (2019) More than energy harvesting-combining triboelectric nanogenerator and flexible electronics technology for enabling novel micro-/nano-systems. *Nano Energy* 57: 851–871. https://doi.org/10.1016/j.nanoen.2019.01.002

7. Sun J, Zhang L, Gong S, et al. (2024) Device physics and application prospect of the emerging high-voltage supply technology arising from triboelectric nanogenerator. *Nano Energy* 119: 109010. https://doi.org/10.1016/j.nanoen.2023.109010
8. Wang X, Chen X, Iwamoto M (2020) Recent progress in the development of portable high voltage source based on triboelectric nanogenerator. *Smart Mater Med* 1: 66–76. https://doi.org/10.1016/j.smaim.2020.07.002
9. Wang ZL, Jiang T, Xu L (2017) Toward the blue energy dream by triboelectric nanogenerator networks. *Nano Energy* 39: 9–23. https://doi.org/10.1016/j.nanoen.2017.06.035
10. Chen J, Yang J, Li Z, et al. (2015) Networks of triboelectric nanogenerators for harvesting water wave energy: A potential approach toward blue energy. *ACS Nano* 9: 3324–3331. https://doi.org/10.1021/acsnano.5b00534
11. Li XF, Berbille A, Wang TY, et al. (2024) Defect passivation toward designing high-performance fluorinated polymers for liquid-solid contact-electrification and contact-electro-catalysis. *Adv Funct Mater* 34: 2315817. https://doi.org/10.1002/adfm.202315817
12. Han K, Luo J, Feng Y, et al. (2020) Self-powered electrocatalytic ammonia synthesis directly from air as driven by dual triboelectric nanogenerators. *Energy Environ Sci* 13: 2450–2458. https://doi.org/10.1039/D0EE01102A
13. Corrielli G, Crespi A, Osellame R (2021) Femtosecond laser micromachining for integrated quantum photonics. *Nanophotonics* 10: 3789–3812. https://doi.org/10.1515/nanoph-2021-0419
14. Lin Z, Hong M (2021) Femtosecond laser precision engineering: From micron, submicron, to nanoscale. *Ultrafast Sci* 2021: 783514. https://doi.org/10.34133/2021/9783514
15. Jia Y, Chen F (2023) Recent progress on femtosecond laser micro-/nano-fabrication of functional photonic structures in dielectric crystals: A brief review and perspective. *APL Photonics* 8: 090901. https://doi.org/10.1063/5.0160067
16. Phan H, Hoa PN, Tam HA, et al. (2021) Q-switched pulsed laser direct writing of aluminum surface micro/nanostructure for triboelectric performance enhancement. *J Sci-Adv Mater Dev* 6: 84–91. https://doi.org/10.1016/j.jsamd.2020.11.003
17. dos Santos A, Sabino F, Rovisco A, et al. (2021) Optimization of ZnO nanorods concentration in a micro-structured polymeric composite for nanogenerators. *Chemosensors* 9: 27. https://doi.org/10.3390/chemosensors9020027
18. Muthu M, Pandey R, Wang X, et al. (2020) Enhancement of triboelectric nanogenerator output performance by laser 3D-Surface pattern method for energy harvesting application. *Nano Energy* 78: 105205. https://doi.org/10.1016/j.nanoen.2020.105205
19. Wang R, Gao S, Yang Z, et al. (2018) Engineered and laser-processed chitosan biopolymers for sustainable and biodegradable triboelectric power generation. *Adv Mater* 30: 1706267. https://doi.org/10.1002/adma.201706267
20. Guo W, Xia Y, Zhu Y, et al. (2023) Laser-induced graphene based triboelectric nanogenerator for accurate wireless control and tactile pattern recognition. *Nano Energy* 108: 108229. https://doi.org/10.1016/j.nanoen.2023.108229
21. Zhu G, Pan C, Guo W, et al. (2012) Triboelectric-generator-driven pulse electrodeposition for micropatterning. *Nano Lett* 12: 4960–4965. https://doi.org/10.1021/nl302560k
22. Zhang Z, Jiang D, Zhao J, et al. (2020) Tribovoltaic effect on metal-semiconductor interface for direct-current low-impedance triboelectric nanogenerators. *Adv Energy Mater* 10: 1903713. https://doi.org/10.1002/aenm.201903713

23. Yang Y, Zhang H, Chen J, et al. (2013) Single-electrode-based sliding triboelectric nanogenerator for self-powered displacement vector sensor system. *ACS Nano* 7: 7342–7351. https://doi.org/10.1021/nn403021m
24. Wang S, Xie Y, Niu S, et al. (2014) Freestanding triboelectric-layer-based nanogenerators for harvesting energy from a moving object or human motion in contact and non-contact modes. *Adv Mater* 26: 2818–2824. https://doi.org/10.1002/adma.201305303
25. Zhang H, Yang Y, Su Y, et al. (2013) Triboelectric nanogenerator for harvesting vibration energy in full space and as self-powered acceleration sensor. *Adv Funct Mater* 24: 1401–1407. https://doi.org/10.1002/adfm.201302453
26. Bae J, Lee J, Kim S, et al. (2014) Flutter-driven triboelectrification for harvesting wind energy. *Nat Commun* 5: 4929. https://doi.org/10.1038/ncomms5929
27. Wang J, Wu C, Dai Y, et al. (2017) Achieving ultrahigh triboelectric charge density for efficient energy harvesting. *Nat Commun* 8: 88. https://doi.org/10.1038/s41467-017-00131-4
28. Qin H, Xu L, Lin S, et al. (2022) Underwater energy harvesting and sensing by sweeping out the charges in an electric double layer using an oil droplet. *Adv Funct Mater* 32: 2111662. https://doi.org/10.1002/adfm.202111662
29. Zhang B, Gao Q, Li W, et al. (2023) Alternating magnetic field-enhanced triboelectric nanogenerator for low-speed flow energy harvesting. *Adv Funct Mater* 33: 2304839. https://doi.org/10.1002/adfm.202304839
30. Chen BD, Tang W, He C, et al. (2017) Ultrafine capillary-tube triboelectric nanogenerator as active sensor for microliquid biological and chemical sensing. *Adv Mater Technol* 3: 1700229. https://doi.org/10.1002/admt.201700229
31. Ying S, Zhang J, Yan K, et al. (2021) Self-powered direct-current type pressure sensor by polypyrrole/metal Schottky junction. *J Phys D Appl Phys* 54: 424008. https://doi.org/10.1088/1361-6463/ac196c
32. Liu J, Wen Z, Lei H, et al. (2022) A liquid-solid interface-based triboelectric tactile sensor with ultrahigh sensitivity of 21.48 kPa^{-1}. *Nano-Micro Lett* 14: 88. https://doi.org/10.1007/s40820-022-00831-7
33. Yang Y, Zhang H, Lin ZH, et al. (2013) Human skin based triboelectric nanogenerators for harvesting biomechanical energy and as self-powered active tactile sensor system. *ACS Nano* 7: 9213–9222. https://doi.org/10.1021/nn403838y
34. Bagchi B, Datta P, Fernandez CS, et al. (2023) Flexible triboelectric nanogenerators using transparent copper nanowires electrodes: Energy harvesting, sensing human activities and material recognition. *Mater Horiz* 10: 3124–3134. https://doi.org/10.1039/D3MH00404J
35. Song T, Jiang S, Cai N, et al. (2023) A strategy for human safety monitoring in high-temperature environments by 3D-printed heat-resistant TENG sensors. *Chem Eng J* 475: 146292. https://doi.org/10.1016/j.cej.2023.146292
36. Qi C, Yang Z, Zhi J, et al. (2023) Enhancing the powering ability of triboelectric nanogenerator through output signal's management strategies. *Nano Res* 16: 11783–11800. https://doi.org/10.1007/s12274-023-5834-4
37. Zou H, Zhang Y, Guo L, et al. (2019) Quantifying the triboelectric series. *Nat Commun* 10: 1427. https://doi.org/10.1038/s41467-019-09461-x
38. Zhang J, Rogers FJM, Darwish N, et al. (2019) Electrochemistry on tribocharged polymers is governed by the stability of surface charges rather than charging magnitude. *J Am Chem Soc* 141: 5863–5870. https://doi.org/10.1021/jacs.9b00297

39. Baytekin HT, Patashinski AZ, Branicki M, et al. (2011) The mosaic of surface charge in contact electrification. *Science* 333: 308–312. https://doi.org/10.1126/science.1201512
40. Sobolev YI, Adamkiewicz W, Siek M, et al. (2022) Charge mosaics on contact-electrified dielectrics result from polarity-inverting discharges. *Nat Phys* 18: 1347–1355. https://doi.org/10.1038/s41567-022-01714-9
41. Wang J, Xu S, Hu C (2024) Charge generation and enhancement of key components of triboelectric nanogenerators: A review. *Adv Mater* 36: 2409833. https://doi.org/10.1002/adma.202409833
42. Wu H, He W, Shan C, et al. (2022) Achieving remarkable charge density via self-polarization of polar high-k material in a charge-excitation triboelectric nanogenerator. *Adv Mater* 34: 2109918. https://doi.org/10.1002/adma.202109918
43. Shin SH, Bae YE, Moon HK, et al. (2017) Formation of triboelectric series via atomic-level surface functionalization for triboelectric energy harvesting. *ACS Nano* 11: 6131–6138. https://doi.org/10.1021/acsnano.7b02156
44. Biegaj KW, Rowland MG, Lukas TM, et al. (2017) Surface chemistry and humidity in powder electrostatics: a comparative study between tribocharging and corona discharge. *ACS Omega* 2: 1576–1582. https://doi.org/10.1021/acsomega.7b00125
45. Wang S, Xie Y, Niu S, et al. (2014) Maximum surface charge density for triboelectric nanogenerators achieved by ionized-air injection: Methodology and theoretical understanding. *Adv Mater* 26: 6720–6728. https://doi.org/10.1002/adma.201402491
46. Li S, Fan Y, Chen H, et al. (2020) Manipulating the triboelectric surface charge density of polymers by low-energy helium ion irradiation/implantation. *Energy Environ Sci* 13: 896–907. https://doi.org/10.1039/C9EE03307F
47. Chen SN, Chen CH, Lin ZH, et al. (2018) On enhancing capability of tribocharge transfer of ZnO nanorod arrays by Sb doping for anomalous output performance improvement of triboelectric nanogenerators. *Nano Energy* 45: 311–318. https://doi.org/10.1016/j.nanoen.2018.01.013
48. Guo QZ, Yang LC, Wang RC, et al. Tunable work function of $Mg_xZn_{1-x}O$ as a viable friction material for a triboelectric nanogenerator. *ACS Appl Mater Interfaces* 11: 1420–1425. https://doi.org/10.1021/acsami.8b17416
49. Feng H, Li H, Xu J, et al. (2022) Triboelectric nanogenerator based on direct image lithography and surface fluorination for biomechanical energy harvesting and self-powered sterilization. *Nano Energy* 98: 107279. https://doi.org/10.1016/j.nanoen.2022.107279
50. Hong D, Choi YM, Jang Y, et al. (2018) A multilayer thin-film screen-printed triboelectric nanogenerator. *Int J Energy Res* 42: 3688–3695. https://doi.org/10.1002/er.4092
51. Zhang C, Zhang L, Bao B, et al. (2022) Customizing triboelectric nanogenerator on everyday clothes by screen-printing technology for biomechanical energy harvesting and human-interactive applications. *Adv Mater Technol* 8: 2201138. https://doi.org/10.1002/admt.202201138
52. Luo J, Fan FR, Jiang T, et al. (2015) Integration of micro-supercapacitors with triboelectric nanogenerators for a flexible self-charging power unit. *Nano Res* 8: 3934–3943. https://doi.org/10.1007/s12274-015-0894-8
53. Jin S, Wang Y, Motlag M, et al. (2018) Large-area direct laser-shock imprinting of a 3D biomimic hierarchical metal surface for triboelectric nanogenerators. *Adv Mater* 30: 1705840. https://doi.org/10.1002/adma.201705840
54. Qi D, Liu Y, Liu Z, et al. (2016) Design of architectures and materials in in-plane micro-supercapacitors: current status and future challenges. *Adv Mater* 29: 1602802. https://doi.org/10.1002/adma.201602802

55. Liu H, Sun Z, Chen Y, et al. (2022) Laser processing of flexible in-plane micro-supercapacitors: progresses in advanced manufacturing of nanostructured electrodes. *ACS Nano* 16: 10088–10129. https://doi.org/10.1021/acsnano.2c02812
56. Liu X, Du D, Mourou G (2002) Laser ablation and micromachining with ultrashort laser pulses. *Ieee J Quantum Elect* 33: 1706–1716. https://doi.org/10.1109/3.631270
57. Wang S, Yang J, Deng G, et al. (2024) Femtosecond laser direct writing of flexible electronic devices: A mini review. *Materials* 17: 557. https://doi.org/10.3390/ma17030557
58. Yang D, Zhang L, Luo N, et al. (2022) Tribological-behaviour-controlled direct-current triboelectric nanogenerator based on the tribovoltaic effect under high contact pressure. *Nano Energy* 99: 107370. https://doi.org/10.1016/j.nanoen.2022.107370
59. Lee YS, Jeon S, Kim D, et al. (2023) High performance direct current-generating triboelectric nanogenerators based on tribovoltaic p-n junction with ChCl-passivated CsFAMA perovskite. *Nano Energy* 106: 108066. https://doi.org/10.1016/j.nanoen.2022.108066
60. Lin J, Peng Z, Liu Y, et al. (2014) Laser-induced porous graphene films from commercial polymers. *Nat Commun* 5: 5714. https://doi.org/10.1038/ncomms6714
61. Xia SY, Long Y, Huang Z, et al. (2022) Laser-induced graphene (LIG)-based pressure sensor and triboelectric nanogenerator towards high-performance self-powered measurement-control combined system. *Nano Energy* 96: 107099. https://doi.org/10.1109/FLEPS53764.2022.9781522
62. Choi KH, Park S, Hyeong SK, et al. (2020) Triboelectric effect of surface morphology controlled laser induced graphene. *J Mater Chem A* 8: 19822–19832. https://doi.org/10.1039/D0TA05806H
63. Zhao P, Bhattacharya G, Fishlock SJ, et al. (2020) Replacing the metal electrodes in triboelectric nanogenerators: High-performance laser-induced graphene electrodes. *Nano Energy* 75: 104958. https://doi.org/10.1016/j.nanoen.2020.104958
64. Yan Z, Wang L, Xia Y, et al. (2021) Flexible high-resolution triboelectric sensor array based on patterned laser-induced graphene for self-powered real-time tactile sensing. *Adv Funct Mater* 31: 2100709. https://doi.org/10.1002/adfm.202100709
65. Yan J, Wang H, Wang X, et al. (2024) High-performance triboelectric nanogenerators with laser-induced graphene pattern for efficient charge transfer. *Appl Surf Sci* 661: 160034. https://doi.org/10.1016/j.apsusc.2024.160034
66. Li JT, Stanford MG, Chen W, et al. (2020) Laminated laser-induced graphene composites. *ACS Nano* 14: 7911–7919. https://doi.org/10.1021/acsnano.0c02835
67. Phipps CR (2007) Laser ablation and its applications, In: Phipps C, *Contributions to Laser ablation*, 1 Eds., New York: Springer, 281–298.
68. Li Y, Zhou X, Qi W, et al. (2020) Ultrafast fabrication of Cu oxide micro/nano-structures via laser ablation to promote oxygen evolution reaction. *Chem Eng J* 383: 123086. https://doi.org/10.1016/j.cej.2019.123086
69. Shiby S, Kaushik S, Gupta P, et al. (2023) Influence of laser wavelength in simultaneous patterning of fluorinated ethylene propylene and copper electrode surface towards performance enhancement of triboelectric nanogenerator. *Energy Technol* 11: 2300482. https://doi.org/10.1002/ente.202300482
70. Lee K, Mhin S, Han H, et al. (2022) A high-performance PDMS-based triboelectric nanogenerator fabricated using surface-modified carbon nanotubes via pulsed laser ablation. *J Mater Chem A* 10: 1299–1308. https://doi.org/10.1039/D1TA08414C
71. Lee K, Han H, Ryu JH, et al. (2023) Laser-driven formation of $ZnSnO_3$/CNT heterostructure and its critical role in boosting performance of the triboelectric nanogenerator. *Carbon* 212: 118120. https://doi.org/10.1016/j.carbon.2023.118120

72. Trinh VL, Chung CK (2017) A facile method and novel mechanism using microneedle-structured PDMS for triboelectric generator applications. *Small* 13: 1700373. https://doi.org/10.1002/smll.201700373
73. Kim D, Tcho IW, Jin IK, et al. (2017) Direct-laser-patterned friction layer for the output enhancement of a triboelectric nanogenerator. *Nano Energy* 35: 379–386. https://doi.org/10.1016/j.nanoen.2017.04.013
74. Cho H, Jo S, Kim I, et al. (2021) Film-sponge-coupled triboelectric nanogenerator with enhanced contact area based on direct ultraviolet laser ablation. *ACS Appl Mater Interfaces* 13: 48281–48291. https://doi.org/10.1021/acsami.1c14572
75. Huang J, Fu X, Liu G, et al. (2019) Micro/nano-structures-enhanced triboelectric nanogenerators by femtosecond laser direct writing. *Nano Energy* 62: 638–644. https://doi.org/10.1016/j.nanoen.2019.05.081
76. Salauddin M, Rana SMS, Sharifuzzaman M, et al. (2022) Laser-carbonized MXene/ZiF-67 nanocomposite as an intermediate layer for boosting the output performance of fabric-based triboelectric nanogenerator. *Nano Energy* 100: 107462. https://doi.org/10.1016/j.nanoen.2022.107462
77. Zhu S, Xia Y, Zhu Y, et al. (2022) High-performance triboelectric nanogenerator powered flexible electroluminescence devices based on patterned laser-induced copper electrodes for visualized information interaction. *Nano Energy* 96: 107116. https://doi.org/10.1016/j.nanoen.2022.107116
78. Qi Y, Kuang Y, Liu Y, et al. (2022) Kirigami-inspired triboelectric nanogenerator as ultra-wide-band vibrational energy harvester and self-powered acceleration sensor. *Appl Energy* 327: 120092. https://doi.org/10.1016/j.apenergy.2022.120092
79. Mishra S, Rakshita M, Divi H, et al. (2023) Unique contact point modification technique for boosting the performance of a triboelectric nanogenerator and its application in road safety sensing and detection. *ACS Appl Mater Interfaces* 15: 33095–33108. https://doi.org/10.1021/acsami.3c04848
80. Park S, Park J, Kim YG, et al. (2020) Laser-directed synthesis of strain-induced crumpled MoS_2 structure for enhanced triboelectrification toward haptic sensors. *Nano Energy* 78: 105266. https://doi.org/10.1016/j.nanoen.2020.105266
81. Nian Q, Saei M, Xu Y, et al. (2015) Crystalline nanojoining silver nanowire percolated networks on flexible substrate. *ACS Nano* 9: 10018–10031. https://doi.org/10.1021/acsnano.5b03601
82. Ryoo G, Lee B, Shin S, et al. (2023) Laser-assisted interfacial engineering for high-performance all-solid-state batteries. *ChemElectroChem* 10: e202300349. https://doi.org/10.1002/celc.202300349
83. Van Hooreweder B, Moens D, Boonen R, et al. (2013) On the difference in material structure and fatigue properties of nylon specimens produced by injection molding and selective laser sintering. *Polym Test* 32: 972–981. https://doi.org/10.1016/j.polymertesting.2013.04.014
84. Trusovas R, Račiukaitis G, Niaura G, et al. (2015) Recent advances in laser utilization in the chemical modification of graphene oxide and its applications. *Adv Opt Mater* 4: 37–65. https://doi.org/10.1002/adom.201500469